



OPEN ACCESS

EDITED BY

Gianluigi Zito,
National Research Council (CNR), Italy

REVIEWED BY

Yulei Wang,
Hebei University of Technology, China
Phillip Booker,
Laser Zentrum Hannover e.V., Germany

*CORRESPONDENCE

Baolai Yang,
✉ yangbaolai1989@163.com
Xiaolin Wang,
✉ chinaphotonics@163.com

[†]These authors have contributed equally to this work

RECEIVED 08 July 2023

ACCEPTED 30 August 2023

PUBLISHED 18 September 2023

CITATION

Meng X, Li F, Yang B, Ye Y, Chai J, Xi X, Wang P, Wu H, Shi C, Zhang H, Wang X and Han K (2023), A 4.8-kW high-efficiency 1050-nm monolithic fiber laser amplifier employing a pump-sharing structure.
Front. Phys. 11:1255125.
doi: 10.3389/fphy.2023.1255125

COPYRIGHT

© 2023 Meng, Li, Yang, Ye, Chai, Xi, Wang, Wu, Shi, Zhang, Wang and Han. This is an open-access article distributed under the terms of the [Creative Commons Attribution License \(CC BY\)](https://creativecommons.org/licenses/by/4.0/). The use, distribution or reproduction in other forums is permitted, provided the original author(s) and the copyright owner(s) are credited and that the original publication in this journal is cited, in accordance with accepted academic practice. No use, distribution or reproduction is permitted which does not comply with these terms.

A 4.8-kW high-efficiency 1050-nm monolithic fiber laser amplifier employing a pump-sharing structure

Xiangming Meng^{1†}, Fengchang Li^{1†}, Baolai Yang^{1,2,3*}, Yun Ye¹, Junyu Chai¹, Xiaoming Xi^{1,2,3}, Peng Wang^{1,2,3}, Hanshuo Wu^{1,2,3}, Chen Shi^{1,2,3}, Hanwei Zhang^{1,2,3}, Xiaolin Wang^{1,2,3*} and Kai Han^{1,2}

¹College of Advanced Interdisciplinary Studies, National University of Defense Technology, Changsha, China, ²Nanhu Laser Laboratory, National University of Defense Technology, Changsha, China, ³Hunan Provincial Key Laboratory of High Energy Laser Technology, National University of Defense Technology, Changsha, China

The power scaling of ytterbium-doped fiber (YDF) lasers emitting at the wavelength range of 1030 nm–1060 nm has been limited by amplified spontaneous emission (ASE), stimulated Raman scattering (SRS) effect, and transverse mode instability (TMI). These effects pose challenges in achieving a high-output power laser within the range of 1030 nm–1060 nm while maintaining a high signal-to-noise ratio. Based on a counter-pumped fiber laser amplifier utilizing our self-developed ytterbium-doped fiber, we have successfully showcased a 4.8-kW laser output at 1050 nm, accompanied by an 85.3% slope efficiency and nearly diffraction-limited beam quality. By effectively applying ASE and TMI, and controlling the Raman Stokes at ~17 dB below the primary signal wavelength, we have achieved optimal performance at the maximum power level. This high efficiency has been attained through a pump-sharing structure combined with cost-effective, non-wavelength-stabilized 976-nm laser diodes.

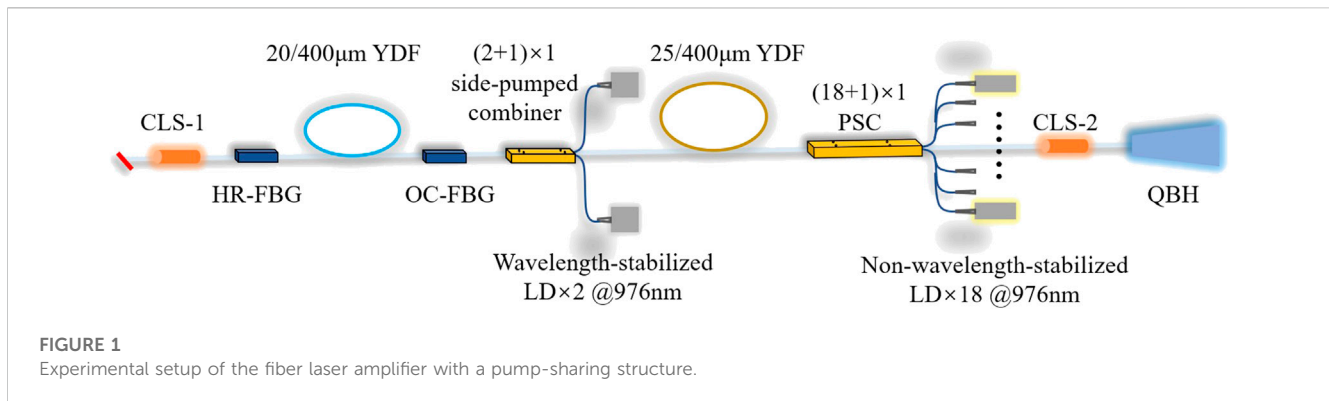
KEYWORDS

short-wavelength fiber lasers, stimulated Raman scattering, amplified spontaneous emission, pump-sharing structure, high power

1 Introduction

High-power fiber lasers have been widely applied in the fields of industrial processing, military defense, and scientific research, owing to high average power, conversion efficiency, and beam quality, and good robustness [1–3]. Short-wavelength fiber lasers attract much attention in spectral combination and non-linear frequency conversion [4–6]. The spectral combining technologies use broadband laser sources for medium output power. Dichroic mirrors are used to combine multiple lasers operating at different wavelengths via transmission and reflection, which greatly decreases the complexity of the experimental system [7–9]. This technology, which utilizes dichroic mirrors, also places a requirement on high-power short-wavelength and long-wavelength lasers [8, 9]. Short-wavelength fiber lasers have the advantage of mitigating transverse mode instability (TMI) because of low quantum defect heating [10].

It is widely recognized that ytterbium-doped fiber (YDF) lasers can deliver high output power within the spectral range of approximately 1030 nm–1100 nm [11]. Compared to fiber lasers in conventional wavelength ranges (1060 nm–1080 nm), short-wavelength fiber lasers



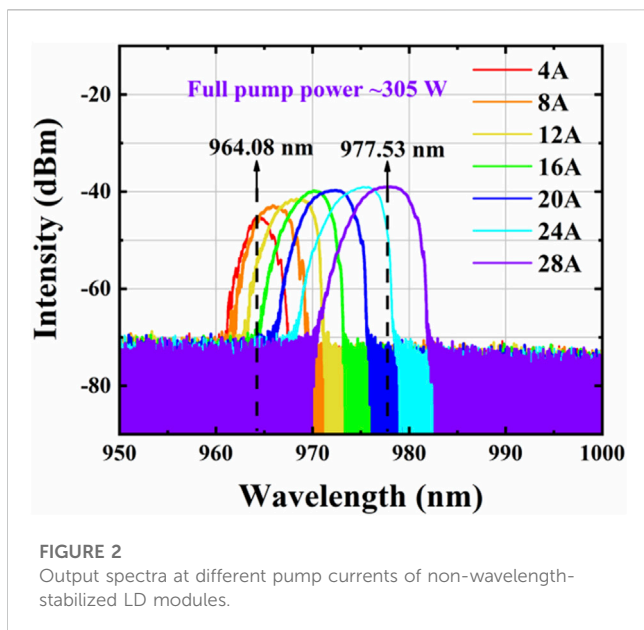
(1030 nm–1060 nm) have larger absorption cross sections. As a result, short-wavelength fiber lasers are more susceptible to the effects of amplified spontaneous emission (ASE) [12, 13]. Moreover, the amplification of short-wavelength fiber lasers is also seriously affected by stimulated Raman scattering (SRS). In recent years, there have been a variety of research studies conducted on high-power fiber lasers at a short-wavelength range [14–19]. Naderi et al. achieved excellent ASE suppression with 40 dB at the power level of 1 kW at 1030 nm, using a preamplifier bandpass filter and optimizing the YDF length in the amplifier stage [16]. Chu et al. demonstrated a 3-kW-level fiber amplifier emitting at 1030 nm with a conversion efficiency of ~70% [15]. A 5.5-m YDF is utilized in the seed laser. An optical isolator is placed between the seed and the amplification stage. The isolator achieves unidirectional transmission and isolation of the optical signal. As a result, the laser output from the seed laser obtains high signal-to-noise ratio (SNR) characteristics. Xu et al. constructed a master oscillation power amplifier (MOPA), and an output power of 2.4 kW at a central wavelength of 1045 nm was achieved [14]. The conversion efficiency of the main amplifier is 80.4%. Zheng et al. constructed a fiber laser at a wavelength of 1050 nm using a pump-sharing structure. The fiber laser achieved an output power of 3.1 kW with a conversion efficiency of 76.7% [19]. The output power of short-wavelength fiber lasers has remained relatively low due to the constraints imposed by ASE and non-linear effects. Additionally, in continuous-wave broadband fiber lasers, power scaling is hindered by thermally induced TMI [20]. Furthermore, it is essential to explore techniques that can improve the relatively low conversion efficiency associated with short YDFs.

In this manuscript, we present the results of a high-efficiency monolithic fiber laser amplifier developed for operation at 1050 nm, utilizing a pump-sharing structure. Various suppression techniques, including ASE, TMI, and SRS, have been employed and optimized to achieve power scaling. The gain fiber utilized in this setup is a tightly coiled, home-made YDF with core and inner cladding diameters of 25/400 μm . In order to increase the TMI threshold, non-wavelength stabilized 976-nm laser diodes (LDs) have been utilized as the pump sources. By appropriately optimizing the lengths of the gain fiber and delivery fiber, we have successfully mitigated the effects of ASE and SRS. The results obtained include an output laser power of 4.8 kW at 1050 nm, with a slope efficiency of 85.3%. When the output power is 4 kW, the beam quality factor (M^2) values in the X and Y directions are 1.56 and 1.43, respectively.

2 Experimental setup

The experimental setup of the 1050-nm monolithic fiber laser amplifier with a pump-sharing structure is shown in Figure 1. It mainly includes a seed and a laser amplifier. The seed laser uses a fiber oscillator structure with counter-pumping. Two wavelength-stabilized 976-nm LDs are injected into the resonant cavity via a (2 + 1) \times 1 side-pumped combiner. Each LD can provide a maximum output power of 250 W at 976 nm. The side-pumped combiner is associated with a linear cavity. The linear cavity consists of a pair of fiber Bragg gratings (FBGs). The core and inner cladding diameters of the FBGs are 20 μm and 400 μm , respectively. The output-coupling fiber Bragg grating (OC-FBG) has a reflectivity of 9.7% and a full width at half maximum (FWHM) of 2.05 nm. The highly reflected fiber Bragg grating (HR-FBG) provides a reflectivity of 99% and an FWHM of 4 nm. The broadband feature of the seed is beneficial to enhance the SRS threshold of the main amplifier stage [21, 22]. The core and inner cladding diameters of the YDF are 20 μm and 400 μm , and the numerical aperture (NA) of the fiber core is 0.065. The total length of YDF is 4.8 m, which has been optimized to avoid ASE by using a relative short gain fiber [19]. The pump absorption coefficient of YDF at the wavelength of 976 nm is 1.2 dB/m. YDF of the seed is coiled on a water-cooled plate with a bending radius of ~50 mm to acquire a nearly single-mode seed laser output. HR-FBG is fused with a cladding light stripper (CLS) to filter out the cladding light, and the tailed fiber of CLS-1 is an 8° angle cleaved to avoid facet reflection.

The pump-sharing structure is employed in this work to enhance the conversion efficiency [23]. In the main amplifier stage, the output fiber of the side-pumped combiner is directly fused with YDF, which has a core/inner cladding diameter of 25/400 μm . The pump absorption coefficient of YDF in the amplifier stage is ~1.07 dB/m at 976 nm. Compared with other gain fibers, the Yb-ion concentration of this home-made gain fiber is decreased. YDF in the main amplifier is also coiled, and the minimum bending diameter is 9 cm. A small bending diameter can filter out higher-order modes (HOM), which have been proven effective for mitigating the TMI [24]. The amplifier stage employs a backward pump/signal combiner (PSC) to constitute a counter-pumping configuration. The PSC has 18 multimode pump ports with core/cladding diameters of 135/155 μm and a core NA of 0.22. Eighteen non-wavelength-stabilized 976-nm LD modules are used for backward pump power, corresponding to a total pump power of ~5500 W. The output spectra at different pump currents of LDs are shown in Figure 2. As the pump current increases, the central



wavelength of LD gradually shifts from 964.08 nm to 977.53 nm. The change in the central wavelength of non-wavelength-stabilized LD with pump current is significant. At a low pump current, the center wavelength stability of LD is poor. At full pump current, the central wavelength of LD tends to stabilize. The full power is ~ 305 W, the central wavelength is 977.53 nm, and FWHM is 4.1 nm. The cooling water temperature of this monolithic fiber laser amplifier is 20°C . The core/inner cladding diameters of the output fiber and the signal fiber of the PSC are $25/400\ \mu\text{m}$ and $25/250\ \mu\text{m}$, respectively. A home-made CLS-2 is utilized to strip the cladding light, and the home-made quartz block holder (QBH) is used to output the laser. QBH has been equipped with protective coatings. These coatings effectively safeguard against optical damage, which may occur during the high-power laser output.

The experimental measurement setup comprises a power meter, an optical spectrum analyzer, a beam quality analyzer, and a photodetector (PD). The output laser, directed through a collimator, is reflected by a high-reflection mirror with reflectivity exceeding 99%. A portion of the transmitted laser is captured using a beam quality analyzer to record the beam quality, while another part is received using the photodetector to capture the temporal signals of the output laser. The specific photodetector used in this experiment is the Thorlabs model “PDA32A2,” which has a bandwidth of 12 MHz. The oscilloscope connected to the photodetector has a bandwidth of 1 GHz. The sensitive area of PD is $13\ \text{mm}^2$, and a small hole with a diameter of 1 mm has been added in front of the sensitive area. The scattered light spectra are measured using an optical spectrum analyzer.

3 Experimental results and discussion

3.1 Optimizing YDF length to mitigate the ASE effect

Suppression of ASE is crucial for successful power scaling. In short-wavelength fiber lasers, reducing the total absorption of the

gain fiber can be used to suppress ASE [14–19]. In our experiment, a fiber laser amplifier with a pump-sharing structure is employed, where the initial seeding laser power is set at 151 W. The length of the germanium-doped fiber (GDF) is defined as the distance from the combiner tail to QBH, and it initially measures 4 m in length. Figure 3A shows the spectrum of the seed laser and the spectra obtained at different YDF lengths when the output power reaches 2800 W. It is evident that the seed laser spectrum is free from ASE light and SRS light. However, at an output power of 2800 W with a pump power of 3191 W, ASE light appears in the spectrum at approximately 1070 nm–1080 nm. Additionally, distinct Raman Stokes signals can be observed. This occurrence of ASE and SRS imposes limitations on further power scaling. The optical SNR of SRS, measured with a 22-m YDF length, is 31.8 dB.

The optimization of the YDF length requires consideration of both the total absorption of YDF and the characteristics of the non-wavelength-stabilized LDs being used [10, 19, 25]. YDF used in the amplifier stage has an absorption coefficient of 1.07 dB/m at 976 nm. When shortening YDF, it is important to balance the suppression of ASE and SRS with the optical-to-optical efficiency of the fiber amplifier. In our experiment, the YDF length of the seed laser is already sufficiently short as ASE is not observed in its spectrum. The seed uses YDF with a short enough length, and no ASE is observed in the seed spectrum. However, if the YDF length is very short, it may result in incomplete absorption of the pump light, leading to the burnout of the CLS. Therefore, we initially reduced the length of YDF in the amplifier stage by 5 m and evaluated the characteristics of the output laser.

As a result of the YDF length reduction, the total absorption of YDF at 976 nm in the amplifier stage decreased from 16.1 dB to 13.2 dB. This reduction still ensures the absorption of the gain fiber for non-wavelength-stabilized 976-nm LDs, thereby achieving high efficiency [10, 25]. The spectrum and the output power versus pump power of the 17-m YDF configuration are shown in Figures 3A, B. The SNR of SRS is improved, measuring 43.2 dB, and ASE in the spectrum has been mitigated. After shortening YDF by 5 m, SNR of both ASE and SRS decreased by approximately 11.4 dB. At a pump power of 3191 W, the output power achieved is 2710 W. Compared to the 22-m YDF configuration, the output power decreases by approximately 113 W under the same pump power. Further shortening of YDF may provide additional benefits in suppressing ASE and SRS, but it will also lead to a reduction in the output power and conversion efficiency. Due to these trade-offs, the length of YDF is no longer optimized in our experiment.

Measuring at 17-m YDF, the output power and corresponding optical efficiency in relation to pump power are illustrated in Figure 4A. The output laser receives an output power of ~ 4020 W with an efficiency of $\sim 79.4\%$. The optical-to-optical efficiency curve is not strictly linear due to non-wavelength-stabilized LDs. As the injection current increases, the central wavelength of LDs shifts toward 977.53 nm, as shown in Figure 2. The total absorption by YDF also increases accordingly. The peaks and valleys of the efficiency curve are caused by the current injection method. Limited by the current source system, the current injection of LDs adopts a hierarchical operation. The power supply is divided into three stages to inject

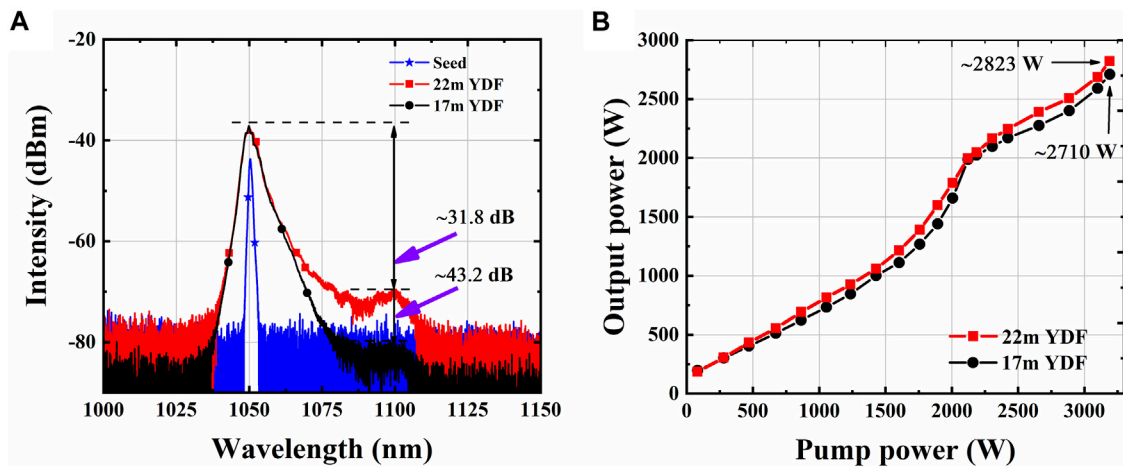


FIGURE 3

(A) Spectra of the seed and the spectra of different YDF lengths at the 2800-W level, and (B) output power versus pump power of 17-m and 22-m YDF.

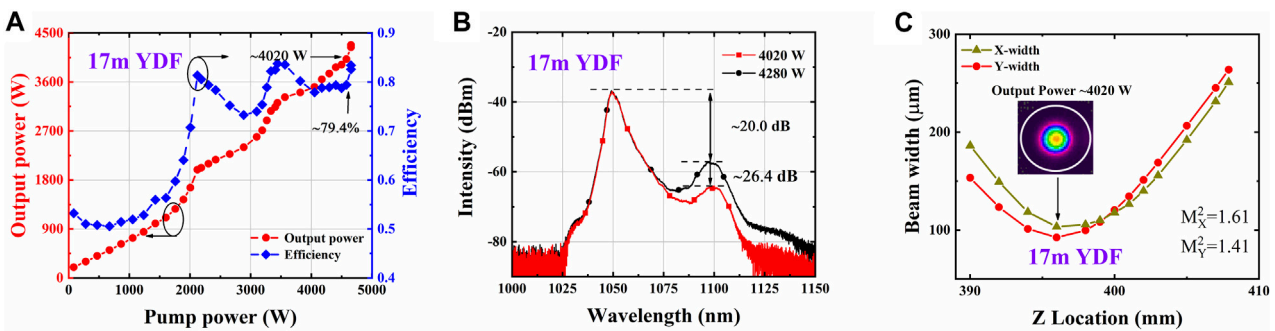


FIGURE 4

(A) Output power characteristics and the corresponding optical-to-optical efficiency of 17-m YDF, (B) spectra at different output power of 17-m YDF, and (C) M^2 factor and beam profile at 4020 W of 17-m YDF.

current. When the first-level power supply is operating at a full load, the power efficiency curve is at the peak position. At this point, the central wavelength of non-wavelength-stabilized LDs is 977.53 nm, and the optical-to-optical conversion efficiency is high. When the second-level power supply current is injected to half of the full load, the power efficiency curve is at the valley, and so on. At this point, the central wavelength of non-wavelength-stabilized LDs is ~969 nm, and the optical-to-optical efficiency is low. Therefore, the optical-to-optical efficiency curve is non-linear. The spectra at different output power of 17-m YDF are shown in Figure 4B. At the output power of ~4020 W, SNR of SRS is ~26.4 dB. The M^2 factor and beam profile at 4020 W are shown in Figure 4C. The inset is the beam profile at the beam waist. The beam quality factor M^2 is 1.61 and 1.41 in the X and Y directions, respectively. Continuing to increase the pump power, when the output power reaches 4280 W, the SNR of SRS is 20.0 dB. By optimizing the YDF length of the amplifier stage, there is an obvious decrease in the ASE intensity near 1080 nm and the SRS intensity near 1100 nm. Further power scaling is limited by SRS.

3.2 Further power scaling to 4.8-kW laser output

Further shortening the YDF length may improve SNR, but the absorption of pump light will also decrease. A 17-m-long YDF can ensure a sufficient absorption of YDF for non-wavelength-stabilized LDs with a wavelength of 976 nm. To ensure a high efficiency of the fiber amplifier, the length of YDF is no longer changed, and optimizing the GDF length is utilized. Reducing the GDF length is beneficial to enhance the SRS threshold. We have truncated the length of GDF by 1.5 m, leaving 2.5 m. This length ensures the fusion of PSC, CLS, and QBH. In order to maintain consistency in the experiment, the output power of the seed is still 151 W. The performance of the amplifier is investigated. The spectra of the seed and the different output power of 2.5 m GDF are shown in Figure 5A. It is shown that the spectrum of the seed is clean without ASE light and SRS light. When the output power is 4260 W, the SNR of SRS is 27.9 dB. Compared with 4-m GDF, the SNR of SRS increases by ~7.9 dB at the same output power level. At the

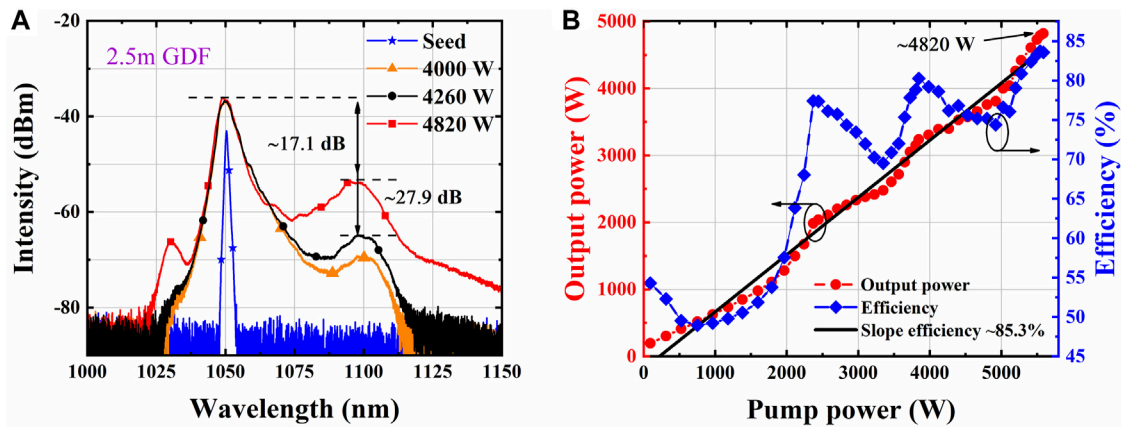


FIGURE 5 Spectra of seed and different output power of 2.5-m GDF, and (B) output power characteristics and the corresponding optical-to-optical efficiency of the fiber amplifier of 2.5-m GDF.

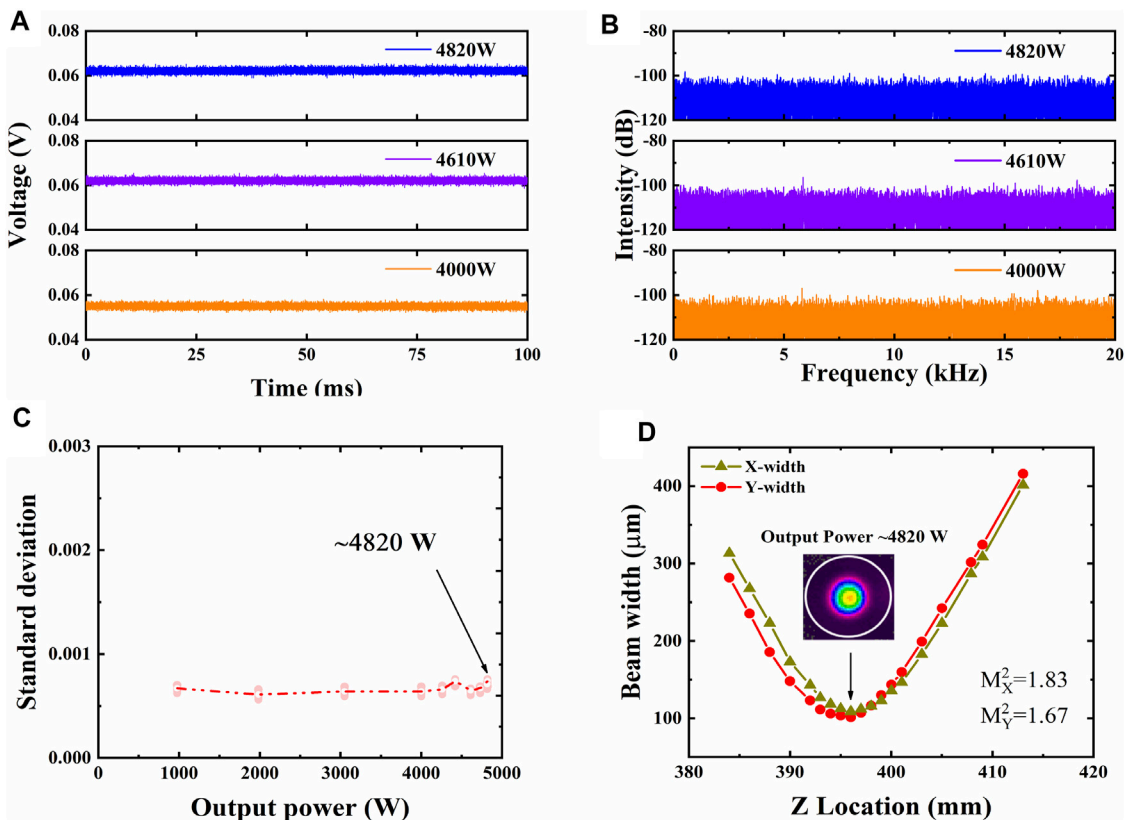


FIGURE 6 (A) Temporal signals at different output powers, (B) corresponding Fourier spectra, (C) STD of the temporal signals at different power levels, and (D) M² factor and beam profile at an output power of 4.8 kW.

maximum output power of ~4820 W, the intensity of SRS is ~17.1 dB lower than the intensity of signal light. There is a small peak with a central wavelength of 1030 nm, which is inferred to be an inter-mode four-wave mixing (FWM) effect [26]. The further increase in power is limited by the non-linear effect and ASE. The

spectral broadening caused by ASE and SRS still requires further attention and improvement. The output power and corresponding optical efficiency in relation to pump power of 2.5 m GDF are illustrated in Figure 5B. The output laser gets a maximum power of ~4820 W with a slope efficiency of ~85.3%. Compared with the

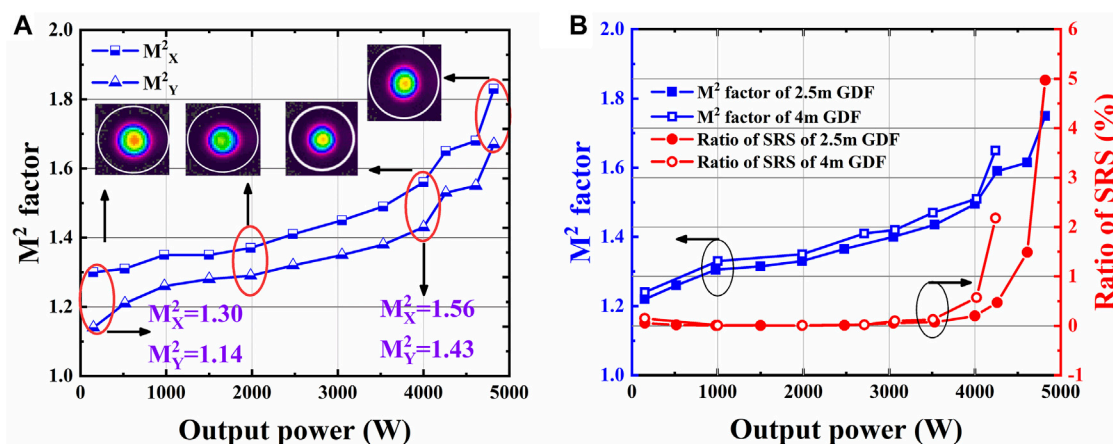


FIGURE 7

(A) Beam quality evolution and corresponding beam profile during the power scaling of 2.5-m GDF, and (B) M^2 factor and ratio of SRS of 2.5-m GDF and 4-m GDF.

conventional MOPA structure, there is no CLS or isolator between the seed and amplifier stage in the pump-sharing structure [19]. When the counter-pump light of the amplifier stage is not completely absorbed by the gain fiber, it can be pumped into the seed stage through the side-pumped combiner. Backward residual pump light increases the power of the seed, further enhancing the output power of the amplifier stage. The corresponding optical-to-optical efficiency also increases accordingly.

Figures 6A, B show the time domain signals and corresponding Fourier spectra at various power levels for the 17-m-long YDF and 2.5-m-long GDF. At output powers of 4 kW, 4.61 kW, and 4.82 kW, there are no noticeable signal fluctuations observed. The corresponding Fourier spectra do not exhibit any distinctive peaks. To quantitatively assess the absence of TMI during high-power amplification, the change in temporal standard deviation (STD) with output power is shown in Figure 6C. If TMI occurs, there would be a sudden increase in the temporal STD [27, 28]. However, the STD remains below 0.001 as the output power increases, indicating the absence of TMI. The high TMI threshold of this fiber amplifier can be attributed to several factors. First, the small bending diameter of the groove filters out HOMs, thus suppressing TMI. Additionally, the short-wavelength nature of the fiber amplifier results in lower quantum defect heating compared to conventional wavelengths, which aids in TMI suppression [29]. Moreover, the 17-m-long YDF with a low absorption coefficient at 976 nm and the use of non-wavelength-stabilized LDs also contribute to the high TMI threshold [25, 30]. Therefore, the demonstrated short-wavelength fiber amplifier exhibits a higher-TMI threshold. The beam quality of the output laser is evaluated using a beam quality analyzer, and the results at an output power of 4.8 kW are presented in Figure 6D. The beam quality factor (M^2) is measured as 1.83 in the x -direction and 1.67 in the y -direction.

Figure 7A shows the evolution of beam quality during the power scaling process, along with the corresponding beam profiles. As the output power of the 1050-nm fiber laser amplifier increases, the beam quality degrades. Below 4.0 kW output power, the beam quality factor M^2 remains below 1.5. However, at an output

power of 4.0 kW, the beam quality factors in the x -direction and y -direction deteriorate to 1.56 and 1.43, respectively. Once the output power surpasses 4 kW, the beam quality rapidly deteriorates. The initial beam quality factor of the seed laser is 1.22, and it increases to 1.75 at the maximum output power of 4.8 kW. Figure 7B illustrates the relationship between the beam quality factor and the ratio of SRS at different lengths of GDF. When the GDF length is 2.5 m or 4 m, the ratio of SRS remains below 0.1% below 4 kW output power. However, beyond 4 kW output power, the ratio of SRS increases significantly. For a GDF length of 4 m and an output power of 4.28 kW, the ratio of SRS is approximately 2.1%. When the GDF length is reduced to 2.5 m and the output power is 4.8 kW, the ratio of SRS reaches approximately 5%.

Figure 7B shows that when the output power is below 4 kW, the beam quality factor M^2 slowly degrades from 1.2 to 1.5. This degradation of beam quality can be considered a result of the thermal effect [31–33]. The injecting seed laser is not strictly single mode. Although HOMs can be partially filtered out by bending loss, residual HOMs are amplified with power scaling. The gradually amplified HOMs lead to slow degradation of beam quality below 4 kW. When the output power of the laser exceeds 4 kW, degradation in beam quality occurs. At this point, there is an abrupt increase in the proportion of SRS power. Figures 6A, B show the temporal signal and the corresponding Fourier spectra at an output power of 4 kW, 4.61 kW, and 4.82 kW, respectively. There is no sign of TMI in 100 m of the normalized time traces. In the range of 0–20 kHz, there is also no signal fluctuation on the Fourier spectra. The results show that TMI has not been triggered. Based on the consistency between the increase in SRS power and the degradation of the beam quality factor, the degradation of beam quality may be caused by SRS [34–36]. The aforementioned results are consistent with the phenomena described in [34, 35]. Limited by experimental conditions, the detailed temporal dynamics at an output power above 4 kW have not been analyzed. The thermal effect may also be involved in the degradation of beam quality greater than 4 kW. It can be determined that shortening the length of GDF within a certain limit can reduce SRS intensity and thereby

improve beam quality. Although the beam quality has degraded to over 1.5 at 4.8 kW, the higher output power with an excellent beam quality and high optical SNR is promising to be achieved by further optimizing the length of the fiber and employing longitudinally varying core diameter active fibers.

4 Conclusion

In this study, we present a high-power 1050-nm fiber amplifier based on a pump-sharing structure. The amplifier utilizes a 25/400- μm YDF with a low absorption coefficient. To effectively mitigate TMI, non-wavelength-stabilized LDs are employed for counter-pumping. By carefully optimizing the lengths of YDF and GDF, both ASE and SRS are effectively suppressed. To achieve a maximum efficiency, we select a 17-m-long YDF and a 2.5-m-long GDF. With this configuration, an impressive output power of 4.8 kW is attained, accompanied by a high slope efficiency of 85.3%. The SNR of the SRS is measured at 17.1 dB at this power level. It is worth noting that the beam quality factor (M^2) remains below 1.5 for output powers below 4 kW but degrades to 1.75 at the maximum output power. This degradation in beam quality can be attributed to thermal effects and the increasing influence of SRS, both of which become more prominent during the power scaling process. Moreover, further increases in the output power are limited due to the presence of SRS and ASE. Nevertheless, this study provides valuable insights and serves as a reference for the development of high-power and high-efficiency 1050-nm fiber amplifiers. It addresses the challenges associated with TMI, SRS, and ASE, and offers potential solutions to enhance the performance of future fiber amplifier designs in this wavelength range.

Data availability statement

The original contributions presented in the study are included in the article/supplementary material; further inquiries can be directed to the corresponding authors.

References

1. Nilsson J, Payne D. High-power fiber lasers. *Science* (2011) 332(6032):921–2. doi:10.1126/science.1194863
2. Jauregui C, Limpert J, Tünnemann A. High-power fibre lasers. *Nat Photon* (2013) 7(11):861–7. doi:10.1038/nphoton.2013.273
3. Richardson D, Nilsson J, Clarkson W. High power fiber lasers: Current status and future perspectives [invited]. *J Opt Soc Am B* (2010) 27(11):B63–B92. doi:10.1364/JOSAB.27.000B63
4. Augst S, Ranka J, Fan T, Sanchez A. Beam combining of ytterbium fiber amplifiers (Invited). *J Opt Soc Am B* (2007) 24(8):1707–15. doi:10.1364/JOSAB.24.001707
5. Fan T. Laser beam combining for high-power, high-radiance sources. *IEEE J Sel Top Quant* (2005) 11(3):567–77. doi:10.1109/JSTQE.2005.850241
6. Guo X, Hou W, Peng H, Zhang H, Wang G, Bi Y, et al. 4.44 W of CW 515 nm green light generated by intracavity frequency doubling Yb:YAG thin disk laser with LBO. *Opt Commun* (2006) 267(2):451–4. doi:10.1016/j.optcom.2006.06.086
7. Chen F, Ma J, Wei JC, Zhu R, Zhou W, Yuan Q, et al. 10 kW-level spectral beam combination of two high power broad-linewidth fiber lasers by means of edge filters. *Opt Express* (2017) 25(26):32783–91. doi:10.1364/OE.25.032783
8. Ma P, Jiang M, Wang X, Ma Y, Zhou P, Liu Z. Hybrid beam combination by active phasing and bandwidth-controlled dichromatic mirror. *IEEE Photon Technol. Lett.* (2015) 27(19):2099–102. doi:10.1109/LPT.2015.2453356
9. He X, Xiao H, Ma P, Zhang H, Xu X, Xiaojun Xu 许. 2.3 kW fiber laser spectral beam combination based on dichromatic mirror. *Infrared Laser Eng* (2021) 50(2):20200385. doi:10.3788/IRLA20200385
10. Tao R, Ma P, Wang X, Zhou P, Liu Z. Study of wavelength dependence of mode instability based on a semi-analytical model. *IEEE J Quan Elect.* (2015) 51(8):1–6. doi:10.1109/JQE.2015.2442760
11. Jeong Y, Nilsson J, Sahu J, Payne D, Horley R, Hickey L, et al. Power scaling of single-frequency ytterbium-doped fiber master-oscillator power-amplifier sources up to 500 W. *IEEE J Sel Top Quant* (2007) 11(3):546–51. doi:10.1109/JSTQE.2007.896639
12. Zhou P, Leng J, Hu X, Ma P, Xu J, Liu W, et al. High average power fiber lasers research progress and future prospect. *Chin J. Lasers* (2021) 48(20):2000001. doi:10.3788/CJL202148.2000001
13. Silva A, Boller K, Lindsay I. Wavelength-swept Yb-fiber master-oscillator-power-amplifier with 70 nm rapid tuning range. *Opt Express* (2011) 19(11):10511–7. doi:10.1364/OE.19.10511

Author contributions

XM and FL: investigation, writing—original draft, and writing—review and editing. BY, YY, and JC: investigation, and writing—review and editing. XX, PW, HW, CS, and HZ: resources, and writing—review and editing. HZ, XW, and KH: supervision.

Funding

This work was supported by the Training Program for Excellent Young Innovations of Changsha (kq2206006), the Fund for Distinguished Young Scholars of Hunan (grant no.2023JJ10057), the National Natural Science Foundation of China (62005315), the Open Research Fund of State Key Laboratory of Pulsed Power Laser Technology, Electronic Countermeasure Institute, and the National University of Defense Technology (SKL2022ZR02).

Acknowledgments

The authors wish to thank Xiaoyong Xu, Tao Song, and Pengfei Zhong for their helpful assistance in the experiment.

Conflict of interest

The authors declare that the research was conducted in the absence of any commercial or financial relationships that could be construed as a potential conflict of interest.

Publisher's note

All claims expressed in this article are solely those of the authors and do not necessarily represent those of their affiliated organizations, or those of the publisher, the editors, and the reviewers. Any product that may be evaluated in this article, or claim that may be made by its manufacturer, is not guaranteed or endorsed by the publisher.

14. Xu Y, Sheng Q, Wang P, Cui X, Zhao Y, Xu H, et al. 2.4 kW 1045 nm narrow-spectral-width monolithic single-mode CW fiber laser by using an FBG-based MOPA configuration. *Appl Opt* (2021) 60(13):3740–6. doi:10.1364/AO.420708
15. Chu Q, Shu Q, Liu Y, Tao R, Yan D, Lin H, et al. 3 kW high OSNR 1030 nm single-mode monolithic fiber amplifier with a 180 pm linewidth. *Opt Lett* (2020) 45(23):6502–5. doi:10.1364/OL.405386
16. Naderi N, Dajani I, Flores A. High-efficiency, kilowatt 1034 nm all-fiber amplifier operating at 11 pm linewidth. *Opt Lett* (2016) 41(5):1018–21. doi:10.1364/OL.41.001018
17. Chu Q, Zhao P, Lin H, Liu Y, Li C, Wang B, et al. kW-level 1030 nm polarization-maintained fiber laser with narrow linewidth and near-diffraction limited beam quality. *Appl Opt* (2018) 57(12):2992–6. doi:10.1364/AO.57.002992
18. Jafari N, Sarikhani S, Chenar R, Eyni Chenar R. A high power 1030 nm ytterbium doped fiber laser with a near diffraction limited quality using a 20/400 μm active fiber. *Laser Phys* (2022) 32(7):075103. doi:10.1088/1555-6611/ac687c
19. Zheng Y, Han Z, Li Y, Li F, Wang H, Zhu R. 3.1 kW 1050 nm narrow linewidth pumping-sharing oscillator-amplifier with an optical signal-to-noise ratio of 45.5 dB. *Opt Express* (2022) 30(8):12670–83. doi:10.1364/OE.456856
20. Zervas M. Transverse mode instability, thermal lensing and power scaling in Yb³⁺-doped high-power fiber amplifiers. *Opt Express* (2019) 27(13):19019. doi:10.1364/OE.27.019019
21. Liu W, Ma P, Lv H, Xu J, Zhou P, Jiang Z. General analysis of SRS-limited high-power fiber lasers and design strategy. *Opt Express* (2016) 24(23):26715–21. doi:10.1364/OE.24.026715
22. Ye Y, Yang B, Wang X, Zhang H, Xi X, Shi C, et al. Experimental study of SRS threshold dependence on the bandwidths of fiber Bragg gratings in co-pumped and counter-pumped fiber laser oscillator. *J Opt* (2019) 21:025801. doi:10.1088/2040-8986/aafa65
23. Meng X, Yang B, Xi X, Wang P, Shi C, Zhang H, et al. 3.5 kW 1050 nm monolithic fiber laser amplifier with near-single-mode. *Acta Optica Sin.* (2023). Available at: <http://kns.cnki.net/kcms/detail/31.1252.O4.20230509.1140.128.html>.
24. Lin H, Tao R, Li C, Wang B, Guo C, Shu Q, et al. 3.7 kW monolithic narrow linewidth single mode fiber laser through simultaneously suppressing nonlinear effects and mode instability. *Opt Express* (2019) 27(7):9716–24. doi:10.1364/OE.27.009716
25. Tao R, Ma P, Wang X, Zhou P, Liu Z. Mitigating of modal instabilities in linearly-polarized fiber amplifiers by shifting pump wavelength. *J Opt* (2015) 17(4):045504. doi:10.1088/2040-8978/17/4/045504
26. Feng Y, Wang X, Ke W, Sun Y, Zhang K, Ma Y, et al. Spectral broadening in narrow linewidth, continuous-wave high power fiber amplifiers. *Opt Commun* (2017) 403:155–61. doi:10.1016/j.optcom.2017.07.005
27. Johansen M, Laurila M, Maack M, Noordeggraaf D, Alkeskjold CJT, Lægsgaard J, et al. Frequency resolved transverse mode instability in rod fiber amplifiers. *Opt Express* (2013) 21(19):21847–56. doi:10.1364/OE.21.021847
28. Otto H, Stutzki F, Jansen F, Eidam T, Tünnermann A, Limpert J, et al. Temporal dynamics of mode instabilities in high-power fiber lasers and amplifiers. *Opt Express* (2012) 20(14):15710–22. doi:10.1364/OE.20.015710
29. Otto H, Modsching N, Jauregui C, Limpert J, Tünnermann A. Wavelength dependence of maximal diffraction-limited output power of fiber lasers. *Proc SPIE* (2015) 9344:16–21. doi:10.1117/12.2076894
30. Smith A, Smith J. Increasing mode instability thresholds of fiber amplifiers by gain saturation. *Opt Express* (2013) 21(13):15168–82. doi:10.1364/OE.21.015168
31. Naderi S, Dajani I, Grosek J, Madden T. Theoretical and numerical treatment of modal instability in high-power core and cladding-pumped Raman fiber amplifiers. *Opt Express* (2016) 24(25):16550–65. doi:10.1364/OE.24.016550
32. Zhang H, Xiao H, Wang X, Zhou P, Xu X. Mode dynamics in high-power Yb-Raman fiber amplifier. *Opt Lett* (2020) 45(13):3394–7. doi:10.1364/OL.393879
33. Huang L, Kong L, Leng J, Zhou P, Guo S, Cheng X. Impact of high-order-mode loss on high-power fiber amplifiers. *J Opt Soc Am B* (2016) 33(6):1030–7. doi:10.1364/JOSAB.33.001030
34. Chu Q, Shu Q, Chen Z, Li F, Yan D, Guo C, et al. Experimental study of mode distortion induced by stimulated Raman scattering in high-power fiber amplifiers. *Photon Res* (2020) 8(4):595–600. doi:10.1364/PRJ.383551
35. Tao R, Xiao H, Zhang H, Leng J, Wang X, Zhou P, et al. Dynamic characteristics of stimulated Raman scattering in high power fiber amplifiers in the presence of mode instabilities. *Opt Express* (2018) 26(19):25098–110. doi:10.1364/OE.26.025098
36. Zhang C, Chu Q, Feng X, Xie L, Liu Y, Li H, et al. Mode evolution of high-power monolithic PM fiber amplifiers in the presence of SRS effect. *IEEE Photonic Tech L* (2022) 34(4):215–8. doi:10.1109/LPT.2022.3148999